



AENSI Journals

Advances in Environmental Biology

Journal home page: <http://www.aensiweb.com/aeb.html>



Improving Power Output Prediction from Ocean Salinity and Temperature Energy Converter using Viscosity Model

Shu Kim Lee¹, Fuei Pien Chee¹, Jedol Dayou¹, Awang Sufiyan Abd. Hamid¹, Ejria Saleh² and HLH Chong³

¹ Energy, Vibration and Sound Research Group (e-VIBS), Faculty of Science and Natural Resources, Universiti Malaysia Sabah, Jalan UMS, 88400, Sabah, Malaysia.

² Borneo Marine Research Institute (BMRI), Universiti Malaysia Sabah, Jalan UMS, 88400, Sabah, Malaysia.

³ Water Research Unit (WRU), Faculty of Science and Natural Resources, Universiti Malaysia Sabah, Jalan UMS, 88400, Sabah, Malaysia.

ARTICLE INFO

Article history:

Received 25 June 2014

Received in revised form

8 July 2014

Accepted 14 September 2014

Available online 27 September 2014

Keywords:

Kinetic power output, water head, viscosity model, density model.

ABSTRACT

Salinity difference between fluids can be utilized and converted to useful power through an underwater hydroelectric power unit, Hydrocratic Generator. The generator system relies on the difference between the osmotic pressure of the incoming fresh water from on-ground reservoir, and the surrounding sea water in the system. In this investigation, additional parameter is introduced which is the temperature difference between fluids; hence the system is known as Ocean Salinity and Temperature Energy Conversion System (OSTEC). With the classical Density Model, there is over estimation of the predicted power output if compared to the experimental power output. Backward numerical extrapolation is performed on the experimental flow rate and found that the experimental water head of incoming water is significantly lower than the theoretical water head. This indicated that the experimental water head of incoming water does sustain a certain amount of head losing during the testing. As a consequence to minimize the prediction error, a refined prediction model is formulated by incorporating the effects of frictional head loss and head loss causing by the number of pipe fittings. Computer simulations are presented in this paper to assess the system as the parameters of system are varied using the refined prediction model.

© 2014 AENSI Publisher All rights reserved.

To Cite This Article: Shu Kim Lee, Fuei Pien Chee, Jedol Dayou, Awang Sufiyan Abd. Hami, Ejria Saleh and HLH Chong, Improving Power Output Prediction from Ocean Salinity and Temperature Energy Converter using Viscosity Model. *Adv. Environ. Biol.*, **8(14)**, 70-77, 2014

1.0 INTRODUCTION

Salinity difference between two fluids has been found useful to electrical power generation. The current practical saline power extraction methods are reverse electrodialysis (RED) [1-3] and pressure-retarded osmosis [4-6]. Both of the methods rely on osmosis process with ion specific membranes. However to solve the technical and durability issues of membranes, Hydrocratic Generator [7] is later introduced to derive the power from the mixing of sea water and low-saline incoming water (or fresh water) without using membranes. It makes use of the upward buoyant force from the mixing of two different saline fluids with same temperature, at a certain vertical depth beneath ocean surface. The authors are recently introduced additional parameter into the system that may further excite the upward buoyant force of the rising mixture, which is the temperature difference between the two fluids. This new system was named Ocean Salinity and Temperature Energy Conversion System or OSTEC [8].

Corresponding Author: Jedol Dayou. University Malaysia Sabah, Energy, Vibration and Sound Research Group (e-VIBS), School of Science and Technology, Jalan UMS 88400 Kota Kinabalu, Sabah, MALAYSIA. Tel: +60-88320000, jed@ums.edu.my.

It was found that the higher fluid velocity can be obtained at the sea water surface when the temperature of the incoming fluid is increased in OSTEC System, while the temperature of sea water is constant. This is because the density of the fluid reduced as the temperature increased. Theoretically, this means higher electrical energy can be harnessed from the system using the turbine rotor. A classic density formulation has been derived based on the density difference between the two fluids to assess the power outcome of OSTEC System. However there is overestimation of power output between the classical prediction and the experimental measurement. As a result, backward numerical extrapolation is performed based on the experimental flow rate of incoming water. By this way, the experimental effective head of incoming water is found and it is lower than the theoretical water head. It is therefore suspected that there are certain amounts of water head losses from the theoretical water head.

To examine the sources of water head losses, the classic formulation is refined by associating the effect of frictional head loss. The new formulation predicts flow rate by considering the dynamic viscosity of the fluid flow. With this formulation, the predicted flow rate is much closer to the experimental flow rate, but it is still moderately overestimate the flow rate. Therefore it is believed that there is still certain amount of unknown head loss where the sources are still under investigation.

Prediction of power output could not be completed without identifying unknown head loss, therefore it is estimated theoretically based on possible source. Unknown head loss is conceived to be related with the number of pipe fittings used in the physical setup. The geometrical construction of pipe fittings or components will influence the velocity and acceleration of fluid flow [9]. As a consequence, the unknown head loss is assumed to proportionate with the number of pipe fittings. It is made that if the pipe loop of the physical setup does not change, therefore the unknown head loss is constant.

With the estimated unknown head loss based on the possible source, a more accurate power assessment on OSTEC system can be performed. In order to determine the unit design for OSTEC full-scale system, this paper is written to perform the kinetic power assessment for OSTEC System when the important parameters are varied, with the consideration of frictional head loss and unknown head loss proportionate to the number of pipe fittings.

2.0 PREDICTED MODEL FORMULATION

Ocean Salinity and Temperature Energy Conversion System (OSTEC) consists of an elevated water reservoir and a pair of sea water submerged vertical tubes where the smaller down-tube channels the incoming water from on-ground reservoir to the bottom of the vertically submerged bigger up-tube. Fig. 1 shows the conceptual design of OSTEC system. The naturally heated incoming water from reservoir is funnelled to one of the up-tube inlets (Point 3) and mix with the surrounding sea water. Water mixture is produced which in principle lighter than sea water and therefore rise upwards to surface (Point 2) due to the buoyant force.

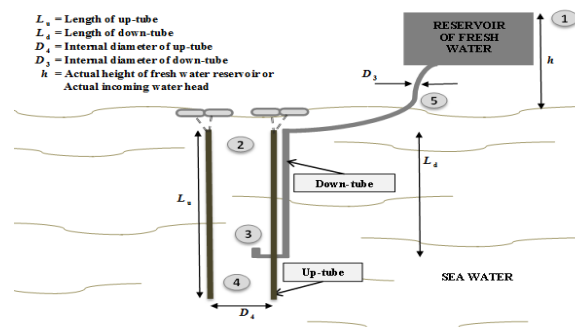


Figure 1. Conceptual design for OSTEC theoretical experiment.

In OSTEC system, salinity and temperature differences between fluids are the main parameters in deriving useful energy from the rising water mixture. It is set that the salinity and temperature of sea water remain constant, and only the salinity and temperature of incoming water from reservoir are varied. Salinity and temperature of incoming water are controlled for becoming less dense and less viscous to induce higher buoyant force so that the formation of water mixture (Point 3) moves upwards with higher flow rate. Kinetic power may be derived from the upward flow of the rising mixture using hydro turbine runner at Point 2 (Figure 1).

Hydrostatic head or known as liquid pressure above a reference datum is essential to provide sufficient pressure for water flowing. It is also stated in the Principle of Energy Conservation, the sum of the pressure head, elevation head, velocity head and head losses accounts for nearly all the energy

encompassed in a unit weight of water flowing through a section of pipe. It is however with the classical Density Model [8], the predicted flow rate of incoming water is far higher than the experimental flow rate [7]. Backward numerical extrapolation using classical density model is therefore performed on the experimental flow rate, to examine the experimental effective head of incoming water.

2.1 Classical Density Formulation

The classical Density Model is derived based on the density difference of fluids to predict power output, with its fluid velocity V_{3_DM} and flow rate Q_{3_DM} as

$$V_{3_DM} = \sqrt{2g\left(\frac{\rho_{PW}}{\rho_3}\right)h_T} \quad (1)$$

$$Q_{3_DM} = A_3 V_{3_DM} \quad (2)$$

where g is the gravitational constant, ρ_{PW} and ρ_3 are the density of pure water at standard temperature and pressure (STP) and incoming water at Point 3, h_T is the total height of the reservoir from the mean sea level or known as theoretical head, and A_3 is the cross sectional area of down-tube. With the experimental velocity of incoming water V_{3_EM} , backward numerical extrapolation is performed to examine the respective effective head h_{e_EM} , using Density Model as

$$V_{3_EM} = \sqrt{2g\left(\frac{\rho_{PW}}{\rho_3}\right)h_{e_EM}} \quad (3)$$

$$h_{e_EM} = \frac{V_{3_EM}^2}{2g} \left(\frac{\rho_3}{\rho_{PW}}\right) \quad (4)$$

As mentioned previously, It is found that the effective head of experimental measurement is significantly lower than the theoretical head. In this sense, it may indicate a certain amount of head loss as

$$h_{L_EM} = h_T - h_{e_EM} \quad (5)$$

For comparison purpose, the calculated amount of head loss h_{L_EM} from experimental results is included into the classical Density Model for providing a good fit with the initial experimental flow rate, and enable better prediction of power output when the other test parameters are varied at similar setting. In view that the source of causing the head loss is still unknown, the calculated head loss is set constant throughout the model simulation.

2.2 Introduction of Viscosity Model

In other sense, changing of fluid temperature and salinity gives an impact to the fluid dynamic viscosity, where dynamic viscosity is analogous to fluid frictional drag effect. In order to further examine the source of the calculated head loss, a new refined formulation is recently introduced by incorporating the effect of frictional head losses. This formulation considers the frictional drag of flowing water with pipe wall roughness and viscous dissipation. It based on the fluid dynamic viscosity μ_1 of incoming water to predict the Darcy friction factor f and thus frictional head losses as

$$h_{f_VM} = f \frac{L}{D_3} \frac{V_T^2}{2g} \quad (6)$$

where V_T , L , and D_3 are the theoretical velocity of incoming water, pipe length and down-tube diameter, respectively. The theoretical velocity is the velocity of incoming water which assumes the total head losses is negligible and therefore its corresponding effective head would be the theoretical head, h_T . The theoretical velocity is given by

$$V_T = \sqrt{2gh_T} \quad (7)$$

The Darcy friction factor f is not constant which depends on the pipe parameter and the velocity of the incoming water flow. It is hence necessary to identify the flow regime of a fluid flow before computing the Darcy friction factor. As a result, Reynolds number N_R is used to characterize the flow regime of incoming water which is written as

$$N_R = \frac{D_3 V_T}{\nu_1} \quad (8)$$

where ν_1 is the kinematic viscosity of the incoming water defined by the ratio of fluid dynamic viscosity μ_1 to the fluid density ρ_1 given as

$$v_1 = \frac{\mu_1}{\rho_1} \quad (9)$$

From the detailed inspection using theoretical velocity of incoming water, it shows that the Reynolds number of the incoming fluid flowing through down-tube is within the range of transitional zone between laminar and turbulent. As a result, the Darcy friction factor will be a function of both the Reynolds number and the relative roughness (e/D) of the pipe. The attribute e is the measurement of absolute roughness of the pipe wall irregular surface whereas D is the pipe internal diameter. It is noted here that the value for e is given for commercial pipe material by the manufacturer. Once N_R and e/D are determined, Swamee-Jain equation is used to get the Darcy friction factor which is

$$f = \frac{0.25}{\left[\log \left(\frac{e/D_3}{3.7} + \frac{5.74}{N_R^{0.9}} \right) \right]^2} \quad (10)$$

Substituting theoretical velocity in equation (7) and Darcy friction factor in equation (10) into equation (6) gives the frictional head loss of the system and therefore effective head of incoming water h_{e_VM} can be determined. With the predicted effective head, fluid velocity of incoming water can be calculated using Viscosity Model as

$$V_{3_VM} = \sqrt{2gh_{e_VM}} \quad (11)$$

By having V_{3_VM} , the flow rate of incoming water from reservoir to the outlet of down-tube (Point 3) can be determined as

$$Q_{3_VM} = A_3 V_{3_VM} \quad (12)$$

2.3 Theoretical Prediction of Unknown Head Losses

The new predicted flow rate of incoming water Q_{3_VM} is closer to the experimental flow rate, if compared to the classically predicted flow rate Q_{3_DM} . It is however that the new predicted flow rate Q_{3_VM} is still slightly higher than the experimental flow rate. Further comparing the frictional head losses with the calculated experimental head losses h_{L_EM} , it is found that besides frictional head losses, there is still other unknown head loss as

$$h_{L_EM} - h_{f_VM} = h_{L_EM_UNKNOWN} \quad (13)$$

As the other head loss is causing from unknown source, it is therefore examined theoretically based on certain possible source during the assessment of power output for OSTEC system. One of the possible sources is the amount of pipe fittings and components used in the physical setup. This type of source relies primarily on the geometrical construction of the component and the impact the construction has on the change of fluid flow velocity and cross flow fluid acceleration. With this possible source, the predicted effective head from Viscosity Model can be written as

$$h_{e_VM} = h_T - (h_{f_VM} + h_{L_EM_UNKNOWN_FITTINGS}) \quad (14)$$

2.4 Kinetic Power Output Prediction

With the including of unknown head losses, the new predicted Q_{3_VM} fits well with experimental measurement. As the incoming water exiting from down-tube outlet (Point 3) and mixes with surrounding sea water, assumption is made that there is complete transfer of kinetic power from incoming water to the surrounding sea water to enable continuous upward flowing of mixing fluid in the up-tube and therefore, the flow rate of sea water flowing through Point 4 can be simplified as

$$Q_4^3 = Q_3^3 \left(\frac{\rho_3}{\rho_4} \right) \left(\frac{D_4^4}{D_3^4} \right) \quad (15)$$

where ρ_4 and D_4 are the density of sea water and internal diameter of up-tube, respectively. It is noted that the formulation in this part of power output prediction is similar for both the classical and refined models. During the transferring of kinetic power from incoming water to surrounding sea water, the salinity and the temperature of the water mixture are changed. By having the flow rate of sea water entering at Point 4, thus the salinity of mixture at Point 2 can be determined as

$$S_2 = (S_4 Q_4 \rho_4) / (Q_3 \rho_3 + Q_4 \rho_4) \quad (16)$$

where S_4 is the salinity of sea water. Because of the two mixing fluids are having different temperature, therefore heat transfer happens between the mixing fluids to achieve heat equilibrium and the temperature of mixture is

$$T_2 = \frac{m_4 C_4 T_4 + m_3 C_3 T_3}{m_4 C_4 + m_3 C_3} \quad (17)$$

Volume flow rate at Point 2 is essential in predicting the kinetic power output. Since the only inlets to the top opening of up-tube (Point 2) are from down-tube outlet (Point 3) and bottom opening of up-tube (Point 4), the volume flow rate at Point 2 is the summation of the flow rate from Point 3 and Point 4 or

$$Q_2 = Q_3 + Q_4 \quad (18)$$

By having the flow rate of water mixture at Point 2, its respective salinity and temperature which determine its density, therefore the kinetic power output for water mixture at the top of up-tube (Point 2) can be predicted as

$$P_2 = 8 \frac{Q_2^3 \rho_2}{\pi^2 D_4^4} \quad (19)$$

3.0 COMPUTER SIMULATION RESULTS

With the Viscosity Model, the predicted flow rate of incoming water $Q_{3,VM}$ and salinity formed at Point 2 $S_{2,VM}$ are crossed check with the respective experimental measurements reported in [7], using similar setting given in Table 1. It is assumed that the pipe material used is polyvinyl chloride (PVC) where its absolute roughness, e is 0.0015 mm. Table 2 presents the comparisons of the two predicted parameters, $Q_{3,VM}$ and $S_{2,VM}$ with the respective reported experimental values, together with the classical Density Model.

Table 1. Parametric Dimensions of OSTEC.

| Parameter | Value(m) |
|--|----------|
| Internal diameter of up-tube, D_4 | 0.150 |
| Internal diameter of down-tube, D_3 | 0.018 |
| Length of up-tube, L_u | 1.500 |
| Length of down-tube, L_d | 1.000 |
| Height of reservoir from mean sea level, h_T | 0.550 |

Table 2. Comparison between prediction from Viscosity Model with the experimental measurement, and together with Density Model.

| | | Q_3 ($e^{-4} m^3 s^{-1}$) | | | S_2 (psu) | | |
|-------------|-------------------------|-------------------------------|-----------------|-----------------|-------------|-------|-------|
| | | EM ^a | VM ^b | DM ^c | EM | VM | DM |
| S_1 (psu) | 0.3 | 2.4 | 2.400 | 2.400 | 34 | 33.08 | 33.08 |
| | $\nabla\%$ ^d | - | 0 | 0 | - | -2.7 | -2.7 |
| | 36 | 2.3 | 2.314 | 2.369 | - | - | - |
| | $\nabla\%$ | - | 0.6 | 3.0 | - | - | - |

^a Reported results from experimental measurement

^b Predicted results from Viscosity Model

^c Predicted results from Density Model

^d Percentage difference of prediction from experimental value

As shown in Table 2 for Viscosity Model, when the low saline incoming water ($S_1 = 0.3$ psu) is used, the predicted flow rate of incoming water $Q_{3,vm}$ channeling from reservoir to Point 3 is $2.4e^{-4} m^3 s^{-1}$, where it is similar with the experimental flow rate, with the expected water head losses of 0.5047 m ($h_{L,VM}$ of 0.3426 m; $h_{L,EM_UNKNOWN_FITTING}$ of 0.1621 m). By using the similar setting, the predicted salinity of water mixture moving up to Point 2 is 33.08 psu with deviation of -2.7% from experimental S_2 . The deviancy may due to the assumption of the complete transfer of kinetic power from incoming fresh water to surrounding sea water without other additional force. In the refined prediction model, it is believed that the additional force due to osmotic pressure has already been included in the formulation in view that it contains the density ratio of low saline fluid to high saline fluid (equation (15)), therefore no other additional force is included into the formulation.

The reservoir is next filled with high saline fluid ($S_1 = 36$ psu) where it has almost the same salinity with sea water. With the similar setting in Viscosity Model, the predicted $Q_{3,VM}$ of the high saline fluid flowing from reservoir to Point 3 is $2.314e^{-4} m^3 s^{-1}$, with deviation of 0.6% from experimental $Q_{3,EM}$. With

the constant value of unknown head losses (same amount of pipe fittings), this indicates that the frictional head losses in Viscosity Model have changed accordingly with the density and dynamic viscosity of the high saline incoming water for better prediction of fluid flow rate. Meanwhile the mixing of the high saline incoming water with the surrounding sea water has not produced continuum rising of water mixture, since the salinity difference between fluids is absolutely lower or neither there.

Through the comparison of predicted values from Viscosity Model with experimental values, the maximum deviation made is just -2.7% from measured value, it is therefore suggested that Viscosity Model is acceptable with small error at least when it is compared with actual measurement. In addition to that, it would be interested to know also the accuracy between Viscosity Model and Density Model. A brief comparison between the deviation percentages of both models is tabulated in Table 2. When the reservoir is filled with low saline incoming water ($S_1 = 0$ psu), the predicted Q_{3_DM} from Density Model has a good agreement with the experimental Q_{3_EM} , with the including of the calculated experimental head losses of 0.5047 m. When the calculated head losses are constant, the predicted Q_{3_DM} of the high saline incoming water is $2.369e^{-4} \text{ m}^3\text{s}^{-1}$, with deviation of 3.0% from experimental Q_{3_EM} . The deviation is rather big if compared to Viscosity Model with 0.6%, is due to the property of frictional head loss in Viscosity Model, where it changes with fluid salinity or density and this result to a closer flow rate. However the change of fluid salinity does not change the calculated head loss in Density Model, it only changes slightly the density ratio in the fluid velocity formulation (equation (1)).

Viscosity Model and Density Model have performed predictions at the same experimental setting, the distinction between their corresponding computer simulations when the tested parameters (salinity difference, temperature difference, down-tube diameter or tube ratio, up-tube diameter and height of reservoir) are further varied would be interested and discussed. During the simulation, temperature and salinity of sea water are fixed at 20 °C and 35 psu respectively whereas temperature and salinity of incoming water from reservoir are varied to examine the effects to kinetic power output. Figure 2(a) and 2(b) present the effect of temperature and salinity to the predicted kinetic power output using Viscosity Model and Density Model respectively, with the setting given in Table 1.

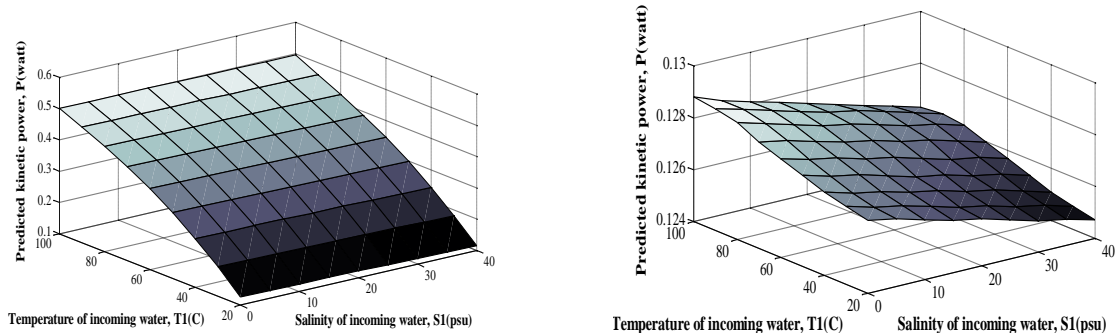


Figure 2. Comparison of the temperature and salinity effect to the kinetic power output using (a) Viscosity Model and (b) Density Model.

It can be seen that from Figure 2(a) the predicted kinetic power increases significantly (overall of about 300%) with higher temperature at all tested salinity, while showing relatively slight changes with fluid salinity (overall of about 10%) at all tested temperature. The dominance of temperature effect in Viscosity Model may be caused by the adherent property of fluid dynamic viscosity. Dynamic viscosity is more temperature dependent rather than salinity; this can be seen through an instance where the reduction of fluid salinity from 40 psu to 0 psu at given temperature of 20 °C results to reduction of dynamic viscosity for only 7.8 % whereas changes of fluid temperature from 20 °C to 100 °C at given salinity of 0 psu results to reduction of dynamic viscosity for 71.9 % [9]. Because of this property, increasing of temperature in Viscosity Model reduces fluid dynamic viscosity largely and therefore lessening much more frictional head loss, and this highly increases incoming flow velocity (equation (11) & (14)) which in turn excites higher kinetic power output of rising water mixture. In view that the amount of pipe fittings is similar with the experimental setting, therefore the similar unknown head loss is used.

On the other hand in Figure 2(b), because of not considering the fluid dynamic viscosity in Density Model, the effect of fluid temperature and salinity are seen to be equally affecting the predicted kinetic power (overall of about 1.6% of each parameter effect). This might due to the property of fluid density by not depending typically on one parameter effect. With respect to this also, change of fluid salinity or temperature do not change the calculated head loss, but only change the density ratio (Equation (1))

slightly, therefore the tested parameters do not present higher effect to the incoming flow velocity and also the predicted kinetic power of rising water mixture (overall of about 1.6%).

Furthermore through equation (6), it can be seen that the frictional head loss is affected by the internal diameter of down-tube. The down-tube diameter is thus varied and simulated to examine the corresponding effect to the remaining effective head. Effective head is the predicted practical head of the incoming water flow during actual experiment, by deducting all the possible expected head losses. It is also noted that these parameter effects can only be tested with Viscosity Model based on equation (6); there is no such relationship in classical Density Model. Figure 3 present the effective head of incoming water when diameter ratios are varied from 2.4 % to 28 % using Viscosity Model, where up-tube diameter is fixed at 0.15 m.

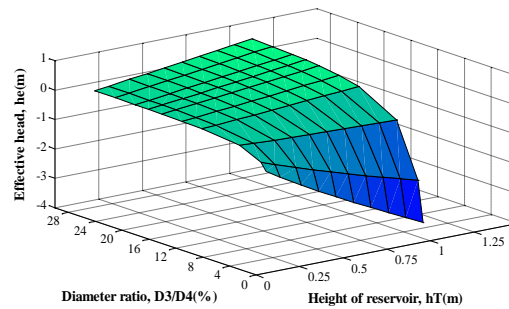


Figure 3. The effective head of incoming water at different diameter ratio and height of reservoir using Viscosity Model.

It is presented that in Figure 3, the percentages of diameter ratio less than 10 % (at fixed up-tube diameter) have negative effective head of incoming water and these heads tend to become more negative with higher height of reservoir. This is causing by the increasing of head loss beyond the cutoff water head when down-tube diameter is reduced to less than 10 % of up-tube diameter. Theoretically it means as the tube diameter become smaller, thus the flow resistance become larger. It is observed also the increasing of reservoir height does not help in adding up the effective head but in reverse results to enlarging of head loss. This may due to that the frictional head loss is velocity dependent and proportionate with higher heights. This finding suggests that tube diameter ratio of less than 10% might not work if for the sake of minimizing the input incoming water, neither it worked by elevating the incoming water reservoir at this absolutely lower diameter ratio.

Differently in the same Figure, effective head increases with those tube diameter ratio more than 10% and tend to become larger with higher elevation of reservoir. This can be explained through equation (6) where head loss reduces with larger down-tube diameter. Due to that the frictional head loss is velocity dependent at various heights, the head loss is in fact increasing with higher heights but its amount is not so significant at larger down-tube diameter and therefore ends up with increasingly positive effective water head with higher heights.

Ocean Salinity and Temperature Energy Converter (OSTEC) works by funneling incoming fresh water into up-tube and get mixed with surrounding sea water to form rising water mixture. This continuum rising force is indeed exciting the entering of sea water into the up-tube through the bottom opening. Therefore, up-tube diameter is proportionate to certain order of sea water flow rate going into up-tube Q_4 as in equation (15). Various diameter ratio more than 10 % at different up-tube diameters are used to simulate the corresponding effects to the kinetic power output as presented in Figure 4 using Viscosity Model. It is once noted here that the amount of pipe fitting used is not changed, therefore the similar unknown head losses is applied in the simulation.

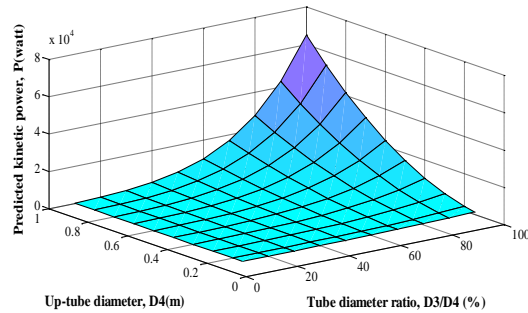


Figure 4. Prediction of kinetic power output at different diameter ratio and up-tube diameter using Viscosity Model.

Further examination of Figure 4 and previous findings in [8] for Density Model shows that it is desirable to have diameter ratio as high as possible so that higher power output can be produced. However, there should be a practical ratio constrained by physical argument. From equation (18), the flow rate at Point 2 is the summation of the flow rate from Point 3 and also Point 4. Thus, adequate space to allow the sea water drift upwards from Point 4 to Point 2 is required. Based on this argument, diameter ratio of 40 % is chosen for further investigation.

Another important point to investigate is on how the height of reservoir (refer Figure 1) affects the power output of the system. This is important when the investigation is performed in full scale experiment at the specific location reported in [8]. To examine this effect, figure 5 is simulated with tube diameter ratio of 40 % and the temperature of sea water and incoming water ($S_1 = 0$ psu) from reservoir are set at 25 °C and 32 °C, respectively. This temperature selection is based on the ambient properties where the future full scale experiment is located. Since that the number of fittings is not changed, the unknown head losses in this case is constant throughout the simulation. Figure 5 presents the effects of reservoir height and together with the up-tube diameter, to the predicted kinetic power, with constant $h_{L_EM_UNKNOWN_FITTINGS}$.

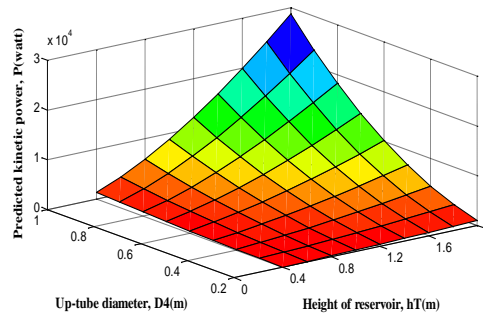


Figure 5. Prediction of kinetic power at different up-tube diameter and height of reservoir using Viscosity Model. The diameter ratio of down-tube to up-tube is fixed at 40%.

Comparison of Figure 5, with previous findings in [8] for Density Model implies that higher kinetic power output can be acquired when the height of reservoir is increased. It is furthermore showing that higher increase rate of power output can be obtained with larger diameter of up-tube. As discussed in Density Model, it is found that up-tube diameter of 0.6 m with length of 7.0 m, at reservoir elevation of 1.8 m, are capable to construct a 10kW electrical power generator unit to meet the power demand of a specified amount of households. Meanwhile for the similar expected outcome in Viscosity Model, a slightly larger setting is predicted through Figure 5, the required up-tube diameter is 0.7 m with length of 7.0 m, applying the same elevation of reservoir as Density Model.

In overall both proposed settings from different model are not differ much except for the up-tube diameter (Viscosity Model: 0.7 m; Density Model: 0.6 m) and down-tube diameter which is 40 % of up-tube diameter (Viscosity Model: 0.28 m; Density Model: 0.24 m). In view that the simulation results from Viscosity Model have relatively closer agreement with reported experimental measurements, it is preferable to pursue the actual experiment with the predicted setting from Viscosity Model.

CONCLUSION

A refined formulation from the classical prediction model is introduced to perform kinetic power output prediction for Ocean Salinity and Temperature Energy Conversion (OSTEC) System. Effects of the frictional head loss of the flowing water with pipe roughness, and head loss based on number of pipe fittings are incorporated in the new prediction model.

With the refined Viscosity Model, the prediction is improved and exhibits lower deviancy from the experimental measurement, if compared with the classical prediction model. Viscosity prediction model shows that higher temperature difference between fluids increases the kinetic power output of the system, if compared to classical model. This is due to the reduction of frictional effect in fluid flow where the coefficient of fluid viscosity is temperature dependent. Larger tube diameter ratio between down-tube and up-tube, bigger up-tube diameter and higher reservoir elevation are found capable to increase the kinetic power output by both prediction models. However in specifically, a limiting boundary is found by the refined model where those tube diameter ratios less than 10 % are unable to produce any useful flow due to its higher water head losing over the theoretical water head.

Parametric design of full-scale experiment predicted by both models to achieve the similar expected outcome are not differ much but just that the refined model predicts slightly larger setting. Instead of up-tube diameter of 0.6 m in classical model, it is now 0.7 m together with tube length of 7.0 m, and 40% of diameter ratio between the down-tube to the up-tube, at an elevation of 1.8 m of reservoir are sufficient to produce 10 kW when the sea water and the incoming water temperature are fixed at 25 °C and 32 °C, respectively. It is preferable to pursue the full-scale experiment with the parametric setting from refined model. With respect to this, future investigation on the performance of full-scale OSTEC System can be conducted and also the source of unknown water head loss can be further examined.

ACKNOWLEDGEMENT

This study is supported by the Ministry of Science, Technology and Innovation of Malaysia under ScienceFund research grant no SCF0089-IND-2013 and Research Priority Area Scheme, University Malaysia Sabah under research grant no SBK0154-ST-0154, and are greatly acknowledged.

REFERENCE

- [1] Branus, E., 2009. Salinity gradient power by reverse electrodialysis: effect of model parameters on electrical power output. *Desalination*, 237(1-3): 378-91
- [2] Hong, J. G., Zhang, W., Luo, J. and Chen, Y. S., 2013. Modeling of power generation from the mixing of simulated saline and freshwater with a reverse electrodialysis system: The effect of monovalent and multivalent ions. *Applied Energy*, 110: 244-51.
- [3] Hong, J. G. and Chen, Y. S., 2014. Nanocomposite reverse electrodialysis (RED) ion-exchange membranes for salinity gradient power generation *J. Membrane Science*, 460: 139-47.
- [4] Kim, H., Choi, J. S. and Lee, S., 2012. Pressure retarded osmosis for energy production: membrane materials and operating conditions *Water Science and Technology*, 65(10): 1789-94
- [5] Thelin, W. R., Sivertsen, E., Holt, T. and Brekke, G., 2013. Natural organic matter fouling in pressure retarded osmosis *J. of Membrane Science*, 438: 46-56
- [6] Helfer, F., Lemckert, C. and Anissimov, Y. G., 2013. Osmotic power with pressure retarded osmosis: Theory, performance and trends – A review *J. of Membrane Science*, 453: 337-58
- [7] Pscheidt, E. and Finley, W., 2003. Deriving useful power from the osmotic potential between solutions Internal Report <<http://www.waderllc.com>> (retrieved on January 13, 2013)
- [8] Lee, S. K., Dayou, J., Awang, S. Abd, H., Saleh, E. and Ismail, B., 2012. A Theoretical Investigation on the Potential Application of Ocean Salinity and Temperature Energy Conversion (OSTEC) *Int. J. of Renewable Energy Research*. 2(2): 326-31
- [9] Franzini, J. B. and Finnemore, E. J. 1997. *Fluid Mechanics with Engineering Applications* (New York: McGraw-Hill)